

Motion Planning and Control for a Tethered, Rimless Wheel Differential Drive Vehicle

Krishna Shankar, Joel W. Burdick
Department of Mechanical Engineering
California Institute of Technology
{krishna, jwb}@robotics.caltech.edu

Abstract—This paper considers motion planning and control problems that are motivated by the design of tethered, extreme terrain robots. We abstract the mobility structure of these systems using a tethered differential drive robot with rimless wheels. We analyze several important issues related to this geometry. First it is shown that this vehicle cannot be modeled deterministically unless an additional degree of freedom relative to the standard differential drive vehicle is provided. The simplest kinematically consistent model is one that allows for slight prismatic motion of the axle, approximating the effects of wheel slip. We show that under mild assumptions, such a vehicle’s reachable set is dense in $SE(2)$, implying local maneuverability. Next we study some of the constraints which the tether places on the vehicle’s motions and derive scaling laws relating wheel and vehicle speeds. Using these results, we provide simple planning and approximate path-following methods that allow tether management. In particular, we consider trajectories produced by solving an optimal control problem to minimize the integral of absolute tether-reeling rate.

I. INTRODUCTION

Background. Some of the highest value sites for future planetary exploration lie in *extreme terrain* that cannot be accessed by flight-ready planetary rovers such as Spirit, Odyssey [1], and Curiosity [2]. Examples of such sites include geological flows on the sides of martian craters [3], and cold traps which may harbor water-ice in permanently shadowed craters on Earth’s Moon [4]. These sites are characterized by steep or verticle slopes, highly rocky terrain, and loose debris.

A number of prototype robotic vehicles have been developed in order to address the challenges of reliable access to steep terrains (e.g. [5]–[9]). We are motivated in particular by the design of the *Axel* rover of Figure 1, developed at The Jet Propulsion Laboratory in collaboration with the California Institute of Technology. *Axel* is a rover with two grouser wheels and a tether fed through a caster arm. The caster arm can rotate about the body to change the tether’s angle of attachment (see [10] for details).

While these vehicles are designed to handle extreme terrain, it is also true that they will need to traverse stretches of open ground while accessing the lips of craters and cliffs, or while operating on the bottom of gulleys and volcanoes. What are the effects of grouser or cleated wheels on the movement of these vehicles—do they have the local controllability needed for precise positioning of scientific instru-

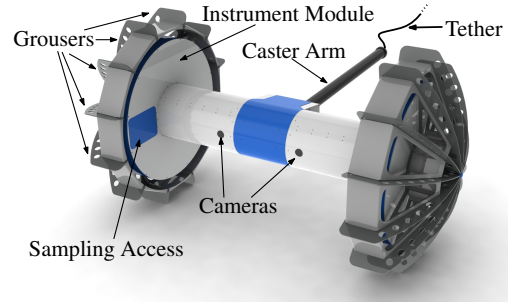


Fig. 1: Axel: An Extreme Terrain Vehicle with Rimless Wheels and a Tether

ments? The use of a tether places a number of restrictions on motion. For example, *Axel*’s on-board winch motor is highly geared to provide a large margin of safety during ascent and descent. While this allows large tether forces to be generated, it also implies that the rate at which the tether can be reeled in or payed out on flat ground is very limited. Which vehicle motions are possible or desirable under strong limits of the tether’s motion? This paper addresses these broad problems by modeling the tethered rover as a differential drive robot with rimless wheels. Since it is very likely that many future robots designed for extreme terrain will use tethers and grouser-like wheels, the methods developed in this paper may find application in other robot systems.

Relation to Prior Work. Control of wheeled vehicles on flat ground is a well studied subject. Shortest paths for a number of bounded-input car-like vehicles were obtained in [11]–[13]. A great deal of work (e.g. [14]–[16]) has addressed the problem of motion planning for non-holonomic wheeled vehicles. Differential drive vehicles are a popular wheeled-robot configuration, and minimum time [17] as well as minimum wheel rotation [18] paths have been found. However, the interaction of grouser-wheels with the terrain cannot be modeled by a classical nonholonomic wheel constraint. Moreover, none of these earlier works incorporated the impact of a tether on the optimality or desirability of specific paths.

The rimless wheel model has been used in a number of human locomotion and biomechanics studies. McGeer [19] introduced the paradigm of human locomotion as a naturally occurring, ‘passive’ motion for a class of mechanical systems, and many works built upon his initial investigation

[20], [21]. These works consider dynamic stability and limit cycles for various ‘gaits’ or speeds of the rimless wheel, and corresponding impacts and energetics in an effort to find the salient characteristics of bipedal locomotion. The modeling and tracking results presented in this paper complement these earlier efforts.

Organization of the Paper. Section II develops a kinematic model for a rimless differential drive vehicle and shows that without at least one more degree of freedom than the standard differential drive vehicle, its motion is inconsistent. We provide control a methodology with a number of desirable characteristics in III, and prove that the vehicle can come arbitrarily close to any goal in SE(2). In IV, motivated by the use of a tether, we show that given a path that can be tracked by piecewise constant inputs, we can select inputs so as to track this path at arbitrary speed. In V we provide planning algorithms for point-to-point motions as well as approximate path following, and tether reeling schedules to accommodate motion in both cases. Simulated experiments and their results are given in VI and the article concludes with VII.

II. MODELING

Rovers designed for rough terrain have wheels without smooth, circular perimeters. Instead they often have grooves, points and sharp edges in order to facilitate traction and climb over rocks (often called grouser or cleated wheels). This class of wheels is approximated by the ‘Rimless Wheel’ shown in Figure 2.

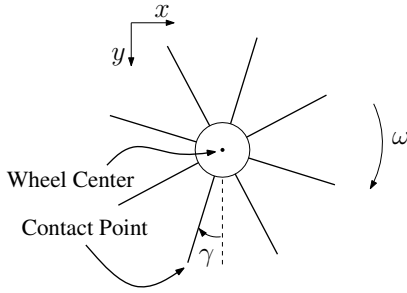


Fig. 2: A Rimless Wheel in 2D

We consider motion on hard ground. Suppose the wheel has n spokes that are uniformly spaced around the perimeter of the circular hub. Then

$$V_c = V_a + \omega \times r_{ac} \quad (1)$$

where V_c is the contact point velocity, V_a is the wheel’s center of mass velocity, ω is the wheel’s angular velocity and r_{ac} is the vector from the wheel’s center to the contact point. Denote the angle between the vertical and the contact point by γ . Let ψ denote the angle that a fixed reference point (e.g. a spoke) on the wheel makes with the vertical. By inspection, notice that

$$\gamma(t) = \left(\psi(t) - \frac{\pi}{n} \right) \bmod \frac{2\pi}{n} - \frac{\pi}{n}$$

so that

$$r_{ac}(t) = \begin{pmatrix} -\rho \sin \gamma(t) \\ \rho \cos \gamma(t) \end{pmatrix}$$

where ρ is the wheel radius. Assuming that the contact does not slip (i.e. $V_c = 0$),

$$V_a = \begin{pmatrix} \dot{x}_a \\ \dot{y}_a \end{pmatrix} = \begin{pmatrix} \omega \rho \cos \gamma(t) \\ \omega \rho \sin \gamma(t) \end{pmatrix} \quad (2)$$

Evolving (2) in time with constant angular velocity results in the motion of Figure 3.

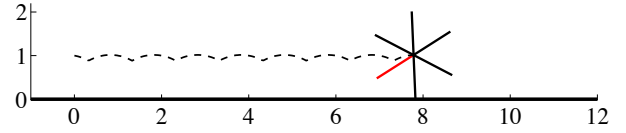


Fig. 3: 2D Rimless Wheel Motion

Proposition 1: A differential drive vehicle with rimless wheels cannot execute a turn without slipping.

In other words, if both wheels of a standard differential drive vehicle are replaced with rimless wheels, one or both of its wheels must *slide* to accommodate turning. Before proving this proposition, we first pursue a modification that allows us to uniquely determine motion and *approximate* the effect of slip.

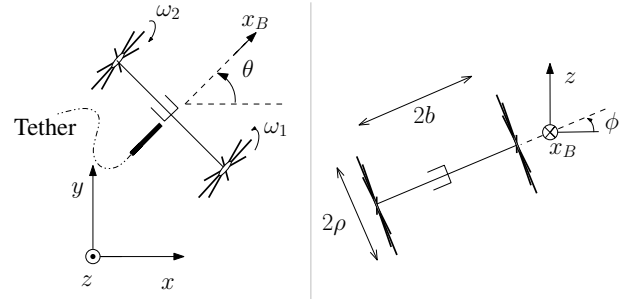


Fig. 4: Coordinate Systems for the Rimless Differential Drive Vehicle. Left: Bird’s eye view. Right: View from behind the vehicle.

To ensure consistency of the kinematic description of the vehicle that arises from the no-slip assumption, we endow the robot with an additional degree of freedom: the distance between the wheels is allowed to vary. This is represented by the addition of a prismatic joint on the axle (figure 4). The modified robot’s state is then given by

$$(x, y, z, b, \theta, \phi) \in \mathbb{R}^4 \times \mathbb{S}^1 \times \mathbb{S}^1$$

where z is positive out of the page, b is the distance between wheel centers, and ϕ is the roll angle (positive about the direction x_B).¹

¹The reader may worry that b may take unreasonably large or small values. For any realistic choice of ρ and initial condition $b(0)$, the maximum range of b is exactly $\left[\sqrt{1/4(\sqrt{3}-2)\rho^2 + b^2(0)}, \sqrt{b(0)^2 + 1/4(2-\sqrt{3})\rho^2} \right]$. In the case of Axel, this means that the wheel span (2.1 m) will deviate from reality by about 1 cm in the worst case.

Vehicle motions are obtained by enforcing no-slip constraints (1) at the spokes' contacts with the ground. After some algebra, we get a set of first order differential equations that govern the vehicle's motion as a function of wheel rates

$$\begin{aligned}\dot{x} &= \frac{\rho}{2} [\cos A(\dot{\phi} \cos \phi \sin \theta + \cos \theta(\dot{\theta} \sin \phi - \omega_1)) + \\ &\quad \cos B(\dot{\phi} \cos \phi \sin \theta + \cos \theta(\omega_2 + \dot{\theta} \sin \phi)) + \\ &\quad \sin \theta(\sin A(\dot{\theta} - \omega_1 \sin \phi) - \sin B(\dot{\theta} + \omega_2 \sin \phi))] \\ \dot{y} &= \frac{\rho}{2} [-\cos A(\dot{\phi} \cos \theta \cos \phi + \sin \theta(\omega_1 - \dot{\theta} \sin \phi)) + \\ &\quad \cos B(-\dot{\phi} \cos \theta \cos \phi + \sin \theta(\omega_2 + \dot{\theta} \sin \phi)) + \\ &\quad \cos \theta(\sin A(\omega_1 \sin \phi - \dot{\theta}) + \sin B(\dot{\theta} + \omega_2 \sin \phi))] \\ \dot{z} &= -\frac{\rho}{2} [\cos \phi(\omega_1 \sin A + \omega_2 \sin B) + \dot{\phi}(\cos A + \cos B) \sin \phi] \\ \dot{\theta} &= \frac{\rho(\omega_1 \cos A + \omega_2 \cos B)}{\rho(\cos A - \cos B) \sin \phi - 2b \cos \phi} \\ \dot{\phi} &= \frac{\rho \cos \phi(\omega_1 \sin A - \omega_2 \sin B) - 2\dot{b} \sin \phi}{2b \cos \phi + \rho(\cos B - \cos A) \sin \phi} \\ \dot{b} &= \frac{-(\omega_1 + \omega_2)\rho^2 \sin(A+B)}{4b}\end{aligned}$$

where

$$A = \left(\int_0^t \omega_1 dt + A_0 + \frac{\pi}{n} \right) \bmod \frac{2\pi}{n} - \frac{\pi}{n} \quad (3)$$

$$B = \left(\int_0^t \omega_2 dt + B_0 + \frac{\pi}{n} \right) \bmod \frac{2\pi}{n} - \frac{\pi}{n} \quad (4)$$

and A_0, B_0 are the initial values of A and B respectively. Now we prove proposition 1.

Proof: Notice that the vehicle *turns* when $\dot{\theta} \neq 0$, and this happens if and only if $\omega_1 \neq -\omega_2$. The kinematic model of the vehicle without the additional prismatic joint is obtained by making b a constant. When this degree of freedom is removed, one finds that the velocities of the contact points are

$$\begin{aligned}V_{c_1} &= \frac{\rho^2(\omega_1 + \omega_2) \sin(A+B)}{4b \cos \phi + 2\rho(\cos B - \cos A) \sin \phi} \begin{pmatrix} -\sin \theta \\ \cos \theta \\ 0 \end{pmatrix} \\ V_{c_2} &= \frac{\rho^2(\omega_1 + \omega_2) \sin(A+B)}{4b \cos \phi + 2\rho(\cos B - \cos A) \sin \phi} \begin{pmatrix} \sin \theta \\ -\cos \theta \\ 0 \end{pmatrix}.\end{aligned}$$

These velocities are well defined, as the denominators are non-zero for any configuration, since $\phi \in [0, \frac{\pi}{2})$ is close to zero and far from $\frac{\pi}{2}$. Observe that when $\omega_1 \neq -\omega_2$, the contact points *cannot* be stationary — $\sin \theta$ and $\cos \theta$ cannot both be zero, and $\sin(A+B)$ is zero only on a set of measure zero (i.e. for at most countably many instants during any interval of time) regardless of A_0, B_0 . ■

III. REACHABILITY ANALYSIS

While operating in harsh conditions, it is important to minimize the possibility of failure. Hence, motion plans should preferably ensure that the robot starts and stops in a *stable stance*, with exactly two spokes of each wheel touching the ground at symmetric angles from the vertical. Note that the vehicle will naturally tend toward such configurations when its actuators are turned off and the wheels are unlocked. This restriction makes plans less sensitive to wheel angle estimates and motor position-control performance.

A concern with such a restriction is that it may limit the configurations which can be reached. For car-like robots, reachability is usually assessed using Chow's Theorem, which says that a system is controllable if and only if the lie algebra generated by its input vector fields is full rank (see [13] for details). Unfortunately it cannot be used here because of the non-smooth nature of the vehicle's kinematics.

If the vehicle motions are limited to a countable set of primitives, the reachable set of states may be considered as a discrete subset of $SE(2)$. If this set is *dense* in $SE(2)$ (i.e. the closure of the reachable set is equal to $SE(2)$) then the vehicle can reach any goal configuration with arbitrary accuracy (for the interested reader, [22] formally presents a notion of reachability for discretely nonholonomic systems e.g. rolling polyhedra). We take the topology on $SE(2)$ to be the product of the standard topologies on \mathbb{R}^2 and \mathbb{S}^1 .

Theorem 1: The subset of $SE(2)$ that is reachable by the rimless differential drive vehicle is dense.

Proof: Let n denote the number of spokes on each wheel. The claim will be proven for $n = 12$, and the same method will apply to many other n 's (oddly, this proof is difficult to generalize with respect to n , but holds for most n). We also assume that $\rho < b(0)$ and $\frac{\rho}{b(0)} \in \mathbb{Q}$.

We need only consider two classes of motion: turning in place (equal wheel speeds) and stepping forward or backward (equal and opposite wheel speeds). In both cases the vehicle is assumed to move from its present stable stance to the nearest stable stance. The euclidean norm of the change in position due to stepping forward or backward Δh is obtained by noticing that in such motion, the robot resembles a regular n -polygonal prism (e.g. for $n = 12$, the robot resembles a dodecagonal prism). One finds that

$$\Delta h = 2\rho \sin \frac{\pi}{n}$$

To compute the net displacement due to a turn $\Delta\theta$, we suppose without loss of generality that $\omega_1 = \omega_2 = \frac{2\pi}{n}$ (Section IV shows that the path of the robot depends only on the ratio of wheel rates, and not their magnitudes), so that the time taken for a turn is one second. To ensure that the initial and final positions are associated with stable stances, and that the motion is associated with a single step, we require that $A_0 = B_0 = -\frac{\pi}{n}$ in (3) and (4), and that time $t \in [0, 1]$. After integrating to find b as a function of time, $\dot{\theta}$ can be

integrated to yield

$$\Delta\theta = \int_0^1 \dot{\theta} dt = -2 \tan^{-1} \left(\frac{\rho}{b(0)} \sin \frac{\pi}{n} \right).$$

First, we show that the set of reachable configurations is dense with respect to rotation (i.e. the robot's heading can be brought arbitrarily close to any direction) using the following lemma:

Lemma 1: If $\frac{\theta \bmod 2\pi}{\pi} \in \mathbb{R} \setminus \mathbb{Q}$, then the set $\{n\theta \bmod 2\pi : n \in \mathbb{N}\}$ is dense in \mathbb{S}^1 (where $\mathbb{S}^1 = [0, 2\pi]_{0 \sim 2\pi}$) [23].

For this lemma to apply, the robot needs to be able to turn by an irrational angle. One can show that $\Delta\theta$ is an irrational angle by using a second lemma:

Lemma 2: [24] Let $\alpha = \frac{2m\pi}{N}$ where $m \in \mathbb{Z}$ and $N \in \mathbb{N}$ have no common factors. Then

- i. $\cos \alpha$ is an algebraic number.
- ii. $\cos \alpha$ is an algebraic number of degree $d > 1$ if and only if $\varphi(N) = 2d$.

Here the arithmetic function $\varphi(N) : \mathbb{N} \rightarrow \mathbb{N}$ is Euler's 'Phi' or 'Totient' function, that specifies the number of naturals smaller than N that have no factors in common with N . \mathbb{Q} is the set of rational numbers.

Observe that $|\Delta\theta| \leq \frac{\pi}{2}$ since $0 < \frac{\rho}{b(0)} \sin \frac{\pi}{n} \leq 1$ and $\tan^{-1}(x) \leq \frac{\pi}{4}$ for $x \in [0, 1]$. Then, notice that it is totally equivalent to show that $\eta = -\frac{1}{2}\Delta\theta$ satisfies lemma 2, since $a \in \mathbb{Q} \Leftrightarrow -\frac{a}{2} \in \mathbb{Q}$. One finds² that

$$\cos \eta = \frac{2}{\sqrt{4 - \frac{\rho^2}{b(0)^2} (\sqrt{3} - 2)}}.$$

This is an algebraic number³ with degree $d = 4$, since its minimal⁴ polynomial is

$$(\beta^4 + 16\beta^2 + 16)x^4 - 8(4 + 2\beta^2)x^2 + 16 = 0$$

where $\beta = \frac{\rho}{b(0)}$. Now we look to Lemma 2, and consider the set $\{N : \varphi(N) = 2d = 8\}$. Explicitly, this set is

$$\{15, 16, 20, 24, 30\}.$$

The rationals less than $\frac{1}{4}$ that have denominators in this set (after simplification) are

$$F = \left\{ \frac{1}{15}, \frac{2}{15}, \frac{1}{16}, \frac{3}{16}, \frac{1}{20}, \frac{3}{20}, \frac{1}{24}, \frac{5}{24}, \frac{1}{30}, \frac{7}{30} \right\}.$$

Therefore $\cos \eta$ and $\cos 2\pi f$ cannot be equal for any $f \in F$ (checked by obtaining exact expressions for the cosines of these angles, observing that none can be equal to $\cos \eta$). Thus, by Lemma 2, η is an irrational multiple of π as is $\Delta\theta$. Using Lemma 1 we conclude that the set of orientations obtained by rotating in place repeatedly is dense in \mathbb{S}^1 .

To show that we can get arbitrarily close to any desired position in translation, first suppose that any rotation can be

²Using the fact that $\cos(\tan^{-1} x) = \frac{1}{\sqrt{1+x^2}}$, and simplifying.

³A number that is the root of a polynomial with rational coefficients.

⁴Check that the polynomial has $\cos \eta$ as a root by calculation. To see that it is minimal (i.e. cannot be factored into other polynomials with rational coefficients), factor the quartic in to a product of 4 linear factors, and realize that neither any of them individually nor any sub-product with each other are polynomials with rational coefficients.

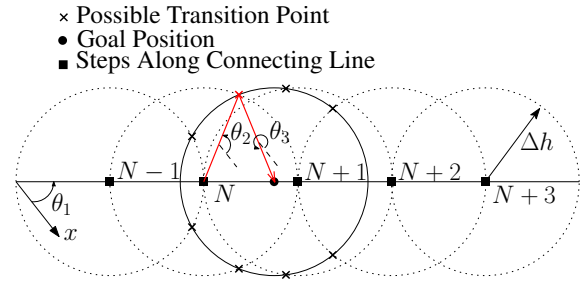


Fig. 5: Reaching an Arbitrary Goal by Stepping

achieved *exactly*, then observe that we can specify a sequence of motions that take us to any goal as follows (see Figure 5):

- Rotate to $\theta = \theta_1$, so that the robot is pointed along the vector from the initial position to the desired position.
- Take a number (N in Figure 5) of steps towards the goal that ensures that the circle of radius Δh centered at this step and the circle of radius Δh centered at the goal intersect.
- Rotate to the angle $\theta = \theta_2$ pointing from the position at the N^{th} step to an intersection of the two circles mentioned above.
- Step forward once to reach the intersection point (it does not matter which one), shown as a red cross.
- Rotate to $\theta = \theta_3$ so that the robot is pointed at the goal.
- Step forward once to reach the goal.

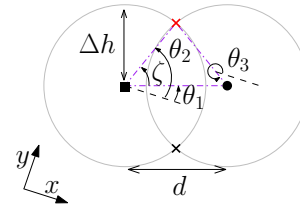


Fig. 6: Geometry of the Last Step

To account for the fact that the robot may not be able to achieve rotations exactly, suppose that instead of rotating to $\theta_1, \theta_2, \theta_3$, it rotates to the erroneous angles $\theta_1 + \delta_1, \theta_2 + \delta_2, \theta_3 + \delta_3$. Without loss of generality, suppose the initial configuration is $(0, 0, 0)$, and that the goal is $(\hat{x}, \hat{y}, \hat{\theta})$. We have

$$\frac{\hat{x}}{\Delta h} = N \cos \theta_1 + \cos \theta_2 + \cos \theta_3$$

$$\frac{\hat{y}}{\Delta h} = N \sin \theta_1 + \sin \theta_2 + \sin \theta_3$$

for some $N \in \mathbb{N}$, by the above construction. The position reached due to erroneous rotation is given by

$$\frac{\tilde{x}}{\Delta h} = N \cos(\theta_1 + \delta_1) + \cos(\theta_2 + \delta_2) + \cos(\theta_3 + \delta_3)$$

$$\frac{\tilde{y}}{\Delta h} = N \sin(\theta_1 + \delta_1) + \sin(\theta_2 + \delta_2) + \sin(\theta_3 + \delta_3).$$

Let the angle between the direction defined by θ_1 and the vector between the N^{th} step and the intersection point be ζ (refer to Figure 6). Using simple geometry, one finds that

$\theta_2 = \theta_1 + \zeta$ and $\theta_3 = \theta_1 - \zeta$, where $\zeta = \tan^{-1} \frac{2\Delta h}{d}$. Then, the squared position error is

$$\begin{aligned} E \triangleq & \frac{1}{\Delta h^2} [(\hat{x} - \tilde{x})^2 + (\hat{y} - \tilde{y})^2] \\ & = 2(1 - \cos(\delta_1))N^2 + 2((1 - \cos \delta_1)(\sin \delta_2 + \sin \delta_3) \\ & \quad + (\cos \delta_2 - \cos \delta_3) \sin \delta_1) \sin \zeta \\ & \quad + [(1 - \cos \delta_1)(\cos \delta_2 + \cos \delta_3) + (\sin \delta_2 + \sin \delta_3) \sin \delta_1] \cos \zeta N \\ & \quad + 2(2 - (\cos \delta_3 + \cos \delta_2) - 4 \cos(\zeta + \frac{\delta_2 - \delta_3}{2}) \sin \frac{\delta_2}{2} \sin \frac{\delta_3}{2}). \end{aligned}$$

It is clear that E can be made arbitrarily small by bounding $\delta_1, \delta_2, \delta_3$. These angles may be made arbitrarily small since the vehicle's rotations are dense. Thus, every open set in the product topology on $SE(2)$ contains a point that can be reached by the vehicle. ■

IV. ACCOMMODATING A TETHER

A tether can be useful (and potentially necessary) to operate on steep terrain. The motor used to spool the tether must be capable of applying large torques, and as a result it operates at an accordingly low top speed. Vehicle motions must be chosen such that the tether is almost taut all the time. One might think to model this reeling constraint explicitly, and solve the corresponding time optimal trajectories between points, but this is analytically intractable and computationally (very) slow. Instead, we make observations about the motion generated by constant inputs and plan motions based on these facts.

Proposition 2: For constant wheel speeds, the standard differential drive vehicle follows a circle of radius between 0 (turning in place) and ∞ (driving in a straight line). This circle depends only on the *ratio* of wheel speeds and initial conditions

This is easily proved by integrating the kinematics with constant inputs, and observing that the resulting configuration path is a circle. Notice that for a fixed ratio of wheel speeds, *scaling the speeds does not affect the circle followed*.

Proposition 3: Suppose that $\dot{\phi}$ and $\dot{\psi}$ are negligible. Then, then Proposition 2 holds for the rimless differential drive vehicle.

This statement likely holds without the assumption, but the proof is tough due to severe non-linearity in the kinematics. The assumption though is not a bad one, as ϕ is small, particularly as n grows large.

Proof: With the assumptions, the kinematics become

$$\begin{bmatrix} \dot{x} \\ \dot{y} \\ \dot{z} \\ \dot{\theta} \\ \dot{b} \end{bmatrix} = \frac{\rho}{2} \begin{bmatrix} -\cos A \cos \theta & \cos B \cos \theta \\ -\cos A \sin \theta & \cos B \sin \theta \\ -\sin A & -\sin B \\ \frac{1}{b} \cos A & \frac{1}{b} \cos B \\ -\frac{\rho}{2b} \sin(A+B) & -\frac{\rho}{2b} \sin(A+B) \end{bmatrix} \begin{pmatrix} \omega_1 \\ \omega_2 \end{pmatrix}.$$

Without loss of generality, suppose that $\omega_1 = M$ and $\omega_2 = \alpha M$ with $M \neq 0$, $0 \leq \alpha \leq 1$. Let $A_0 = B_0 = -\frac{\pi}{n}$. Let $\dot{\theta}_M(t)$ be the rate of change of θ associated with a particular

value of M . Using simple calculus, it can be shown that

$$\begin{aligned} \dot{\theta}_M(t) &= \frac{M\rho}{2b(t)} \left(\cos \left(Mt \bmod \frac{2\pi}{n} - \frac{\pi}{n} \right) \right. \\ & \quad \left. + \alpha \cos \left(M\alpha t \bmod \frac{2\pi}{n} - \frac{\pi}{n} \right) \right) \\ &= M\dot{\theta}_1(t/M). \end{aligned}$$

Integrating with respect to $\tau = Mt$, one finds that $\theta_M(t) = \theta_1(t/M)$. Using a similar approach, one can show that position as a function of time satisfies

$$\begin{aligned} x_M(t) &= x_1(t/M) \\ y_M(t) &= y_1(t/M) \\ z_M(t) &= z_1(t/M). \end{aligned}$$

That is, the paths of the vehicle for different values of M are the same provided the time allocated is scaled appropriately in each case. ■

Let the distance of the vehicle from the origin (the anchor point for the tether) be given by $r(t)$. Then

$$\dot{r} = \frac{x\dot{x} + y\dot{y} + z\dot{z}}{\sqrt{x^2 + y^2 + z^2}}.$$

Corollary 1: For a given path associated with a wheel speed ratio, scaling the wheel speeds results in the same scaling of $\dot{r}(t)$ over the path. More generally, if p is the distance to an arbitrary point fixed with respect to the robot, then the same fact holds for $\dot{p}(t)$.

This means that the rate at which a tether attached *anywhere on the robot* must be reeled in or out scales with the wheel speed, provided the ratio of the wheel speeds remains fixed. This fact implies that a given path generated by piecewise constant inputs and the reeling rates on that path are independent — *the path can be followed with arbitrarily low spooling rates*.

V. PLANNING, PATH FOLLOWING AND OPTIMAL CONTROL

We will detail two simple methods for controlling robot motions. The first provides a means to go from one configuration to another using a set of motion primitives. The second allows the robot to follow a parametrized path. Applying the methods, one obtains a schedule of inputs and tether reeling rates. If, in each of the scenarios, the scaling step is done carefully, then the resulting piecewise constant rates can be tracked easily in practice by tuned motor velocity-controllers.

Note that this method works whether the tether is attached at the origin of the vehicle-fixed frame, or to an appendage that is fixed with respect to this frame (e.g. held by a caster arm as is the case with the Axel Rover). The spokes of the wheels cause the rate of change of distance to the vehicle (or any point fixed on the vehicle) to change in a jagged an discontinuous manner. As a result, it is hard to spool the tether to complement motion exactly.

A. Paths Between Configurations Using Fixed Primitives

We assume that a set of motion primitives

$$\{P_i \mid i = 1 \dots N\}$$

are generated using *constant wheel speeds* (i.e. each primitive is an arc, a straight line, or a turn in place). For each primitive, obtain a time parametrization of the trajectory obtained by applying the primitive at the initial condition

$$(x, y, z, \theta, \phi, b)|_{t=0} = (0, 0, 0, 0, 0, b(0))$$

We also assume a cost function $f : (i, x, y, \theta) \rightarrow \mathbb{R}_{\geq 0}$ is specified, that assigns the cost of using primitive i starting at (x, y, θ) .

Assume that the vehicle starts at the origin, and is required to reach a point $(x_g, y_g, \theta_g) \in \text{SE}(2)$, to an accuracy defined by a euclidean ball of radius ϵ_p centered at (x_g, y_g) and the interval of size ϵ_θ centered at θ_g . By Theorem 1, a path from any starting point in $\text{SE}(2)$ to this set exists. Therefore, dynamic programming (e.g. Dijkstra's Algorithm) can be used to obtain the path and the associated primitive sequence to reach the goal set that minimizes accumulated cost. Once this path is found, the tether reel rate associated with the path, $R(t)$ can be found exactly. Then, the speeds and time allocated to each primitive are scaled to ensure that the reel motor is not saturated (by Proposition 3, the path taken will be the same).

In general, the reeling rate as a function of time is not a pleasant function, so the tether motor is made to slightly overcompensate vehicle motion as follows: Let R_{\max} be the maximum rate that the tether motor can spin at. The range $[-R_{\max}, R_{\max}]$ is quantized to get k tether motor operating rates, $O = \{R_1, R_2 \dots, R_k\}$ where $R_1 = -R_{\max}$ and $R_k = R_{\max}$. Thereafter, the following method is applied to select reel rates as a function of time

- Discretize time (the resolution of the discretization is a design parameter).
- For each time t , compute the overcompensatory reel rate

$$\bar{R}(t) = \begin{cases} 0 & \text{reel rate is zero} \\ \min_{i \in \{1, \dots, k\}} \{R_i \mid R_i \geq R(t)\} & \text{otherwise} \end{cases}$$

In this way, we obtain a schedule of reeling rates and a sequence of control inputs to go from point to point. After the motions have been executed, because the reeling schedule overcompensates, the tether must be reeled slightly until taut using simple tension feedback.

B. Path Following

Suppose that there is a particular path defined by

$$\sigma : [0, \alpha] \rightarrow \text{SE}(2)$$

(i.e. for $\tau \in [0, \alpha]$, $\sigma(\tau) = (x(\tau), y(\tau), \theta(\tau))$) for the vehicle to follow, such that the parametrization is *regular* (see [25] for a definition and background), and such that the derivatives of the trajectory with respect to the parameter are known (or can be approximated well using finite differences). Then we

may *reparametrize* the curve with respect to arc length, an infinitesimal element of which we define by

$$ds = dx^2 + dy^2 + dz^2 + db^2 + (d\theta^2 + d\phi^2)b^2.$$

We want to find piecewise constant inputs to follow the path approximately, and to do this we exploit Proposition 3. Suppose that the vehicle traverses the path in such a way that $\frac{ds}{dt}$ is constant. This means

$$\frac{ds}{dt} = \frac{(\omega_1^2 + \omega_2^2)\rho^2[8b^2 + \rho^2 - \rho^2 \cos(2(A+B))]}{16b^2} = \text{constant}. \quad (5)$$

To make things simpler, ignore the effect of the time-varying cosine term in (5), which is very small compared to other terms (it is easily added back in by integration to get motion as a function of time). We obtain a piecewise constant input approximation of the path as follows:

- Obtain samples along the path of the derivatives and values of the vehicle state (with respect to arc length)
- For each sample s_i and corresponding path and derivative values, solve for ω_1 and ω_2 satisfying

$$\frac{(\omega_1^2 + \omega_2^2)\rho^2[8b^2 + \rho^2]}{16b^2} = 1 \quad (6)$$

$$\frac{\omega_1 + \omega_2}{2b} = \left. \frac{d\theta}{ds} \right|_{s_i} \quad (7)$$

so that

$$\begin{pmatrix} \frac{(\omega_1 + \omega_2)}{2} \cos(\theta(s_i)) \\ \frac{(\omega_1 + \omega_2)}{2} \sin(\theta(s_i)) \end{pmatrix} \cdot \begin{pmatrix} x(s_i) \\ y(s_i) \end{pmatrix} \geq 0. \quad (8)$$

We require (8) because there are two solutions to the system of equations given by (6) and (7), and we select the one with the right local curvature.

- Motion due to these constant inputs is integrated to obtain $R(t)$ (or $R(s)$) as in section V-A.
- Wheel speeds (and corresponding allocated times) are scaled to ensure that the tether reeling motor is not saturated. This can be a global scaling, whereby all inputs are scaled by the same factor, or a piecewise scaling. Again, $\bar{R}(t)$ is selected (see section V-A) to overcompensate vehicle motion.
- After motion is complete, a small amount of reeling using tension feedback is done to remove remaining slack.

VI. SIMULATIONS

A. Example Using Motion Primitives

We select our primitives to be a set of straight lines and arcs, as shown in Figure 7. The forward and backward primitives (straight lines) are generated by taking a single step, with equal and opposite wheel speeds. The arcs are generated by selecting one wheel speed to be five times (in general a whole number $\lambda \in \mathbb{N}$) of the other in magnitude, allowing all sign combinations. In order to ensure that the vehicle goes from stable stance to stable stance, the slower spinning wheel takes one step, while the other wheel takes 5

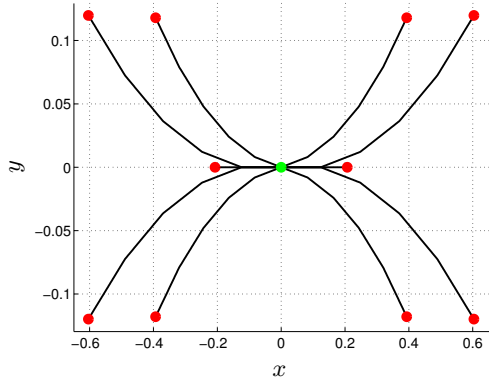


Fig. 7: Motion Primitives

(in general λ) steps. Our task is to plan a path from $(0, 0, 0)$ to an open ball centered at $(3, 2, 0)$. In this case, the cost assigned to a given primitive is the sum of the euclidean distance to its end point and the net angle change multiplied by b . ϵ_p is set to 0.2 and ϵ_θ is set to 10 degrees. The resulting shortest path is shown in Figure 8. We suppose the maximum

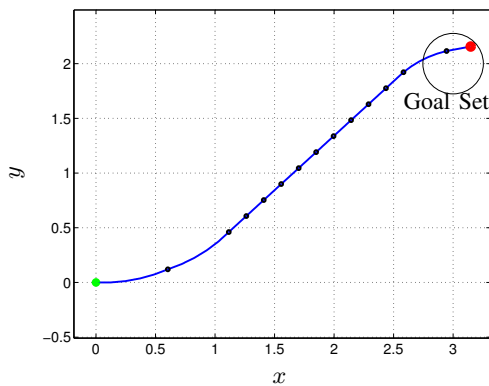


Fig. 8: Shortest Path

allowable reel rate is 0.25, and scale wheel speeds and time for each step of the path accordingly (scaling the wheel speeds does not change the path). The unscaled and scaled reel rates are shown in Figure 9. Notice that the unscaled rate exceeds the spooling limit.

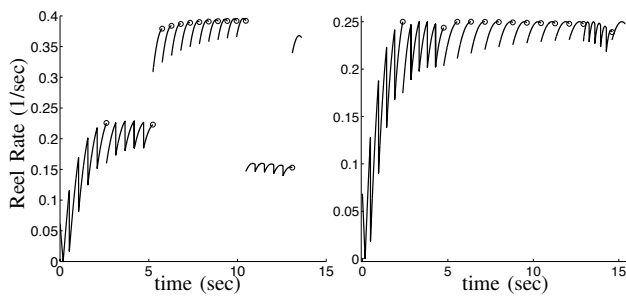


Fig. 9: Reel Rates. Left: Unscaled. Right: Scaled

B. Path Following: Optimal Trajectory

We apply the method of section V-B to approximately follow the path obtained by solving an optimal control problem for the *standard differential drive vehicle*, whose motion

model is considerably simpler and amenable to computation. The path following method of the previous section is then applied to this solution. Consider the problem⁵

$$\begin{aligned} & \text{minimize} \int_0^T R(t)^2 dt \\ & \text{subject to} \quad \dot{q} = f(q, u) \\ & \quad q(0) = q_0, q(T) = q_f \end{aligned} \quad (9)$$

where f represents the vehicle's equations of motion, q the vehicle state, u the inputs and R the tether rate (proportional to the rate of change of radial distance to the vehicle from the origin or anchor point). For the standard differential drive vehicle, the state is given by $q = (x, y, \theta)$. In the example below we seek a path from $q(0) = (2, 2, \pi/3)$ to $q(30) = (0, 0, 0)$. The path produced by the solving the optimal control numerically (using pseudospectral transcription, [26]) is shown in red in Figures 10 and 11. Corresponding control inputs, reel rates and reeling schedules are shown in Figures 12 and 13 respectively. Note that we assume the tether reel has a fixed radius of 1, and that the maximum reeling rate is 0.25 meters per arc length (arc length is proportional to time).

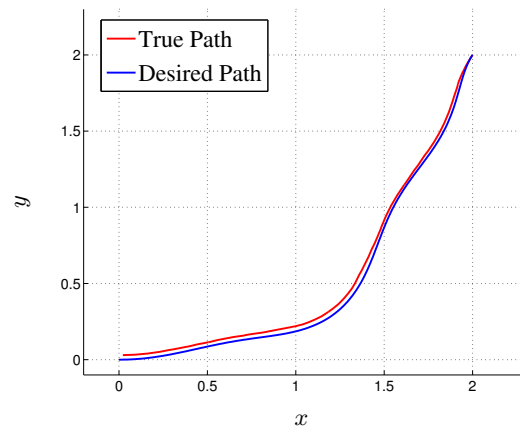


Fig. 10: Path Following: x vs y

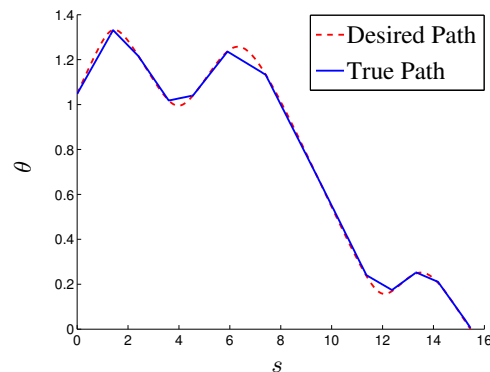


Fig. 11: Path Following: θ vs Arc Length

⁵This problem cannot be solved analytically using pontryagin's maximum principle.

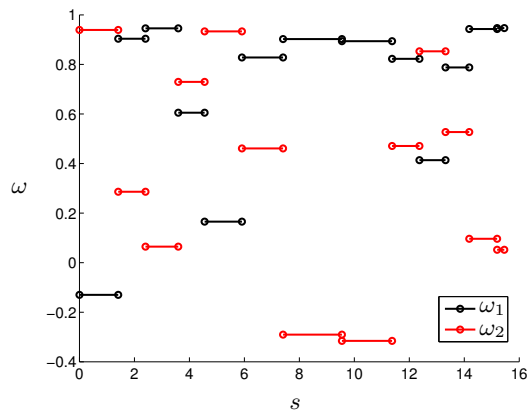


Fig. 12: Path Following: Piecewise Constant Inputs

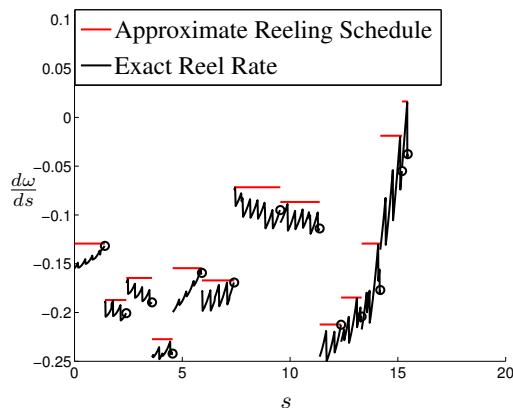


Fig. 13: Path Following: True Reel Rate and According Reel-Rate Schedule

VII. CONCLUSION AND FUTURE WORK

We presented a kinematic model of a tethered differential drive rover with rimless wheels, studied its mobility and obtained principles to motivate the control architecture for a tethered extreme terrain vehicle. We introduced two simple planning methods, one that uses motion primitives to go from point to point, and another that follows parametrized paths by approximation. In both cases, we provide a means for tether management.

The methods presented in this paper will be implemented and experimentally tested on the Axel Vehicle.

REFERENCES

- [1] NASA. (2011) Mer mission. [Online]. Available: http://www.nasa.gov/mission_pages/mer/
- [2] NASA/JPL. (2012) Mars science laboratory. [Online]. Available: <http://mars.jpl.nasa.gov/msl/mission/>
- [3] NASA. (2011) Nasa explores the red planet. [Online]. Available: http://www.nasa.gov/mission_pages/mars/images/pia0902.html
- [4] A. Colaprete, P. Schultz, J. Heldmann, D. Wooden, M. Shirley, K. Ennico, B. Hermalyn, W. Marshall, A. Ricco, R. C. Elphic *et al.*, "Detection of water in the Icross ejecta plume," *Science*, vol. 330, no. 6003, pp. 463–468, 2010.
- [5] P. Perjanian, C. Leger, E. Mum, B. Kennedy, M. Garret, H. Aghazarian, S. Faritor, and P. Schenker, "Distributed control for a modular, reconfigurable cliff robot," in *Proc. IEEE Int. Conf. on Robotics and Automation*, vol. 4. IEEE, 2002, pp. 4083–4088.

- [6] J. Bares and D. Wettergreen, "Dante ii: Technical description, results, and lessons learned," *The International Journal of Robotics Research*, vol. 18, no. 7, pp. 621–649, 1999.
- [7] U. Bremen. (2013) Cesar: Crater exploration and sample return. [Online]. Available: <http://cesar.dfki-bremen.de/>
- [8] B. L. University. (2013) Cosmic materials space research group. Budapest, Hungary. [Online]. Available: <http://planetologia.elte.hu/>
- [9] K. Yoshida, K. Nagatni, T. Ito, and H. Kinoshita, "Wheels, tracks and reciprocal walking," in *Proceedings of the ICRA'11 Space Robotics Workshop*, 2011.
- [10] I. A. Nesnas, J. B. Matthews, P. Abad-Manterola, J. W. Burdick, J. A. Edlund, J. C. Morrison, R. D. Peters, M. M. Tanner, R. N. Miyake, B. S. Solish *et al.*, "Axel and duaxel rovers for the sustainable exploration of extreme terrains," *Journal of Field Robotics*, 2012.
- [11] L. Dubins, "On curves of minimal length with a constraint on average curvature, and with prescribed initial and terminal positions and tangents," *American Journal of Mathematics*, pp. 497–516, 1957.
- [12] J. Reeds and L. Shepp, "Optimal paths for a car that goes both forwards and backwards," *Pacific Journal of Mathematics*, vol. 145, no. 2, pp. 367–393, 1990.
- [13] H. Sussmann and G. Tang, "Shortest paths for the reeds-shepp car: a worked out example of the use of geometric techniques in nonlinear optimal control," *Rutgers Center for Systems and Control Technical Report*, vol. 10, pp. 1–71, 1991.
- [14] R. M. Murray and S. S. Sastry, "Nonholonomic motion planning: Steering using sinusoids," *Automatic Control, IEEE Transactions on*, vol. 38, no. 5, pp. 700–716, 1993.
- [15] J.-P. Laumond, P. E. Jacobs, M. Taix, and R. M. Murray, "A motion planner for nonholonomic mobile robots," *Robotics and Automation, IEEE Transactions on*, vol. 10, no. 5, pp. 577–593, 1994.
- [16] J. Barraquand and J.-C. Latombe, "On nonholonomic mobile robots and optimal maneuvering," in *Intelligent Control, 1989. Proceedings., IEEE International Symposium on*. IEEE, 1989, pp. 340–347.
- [17] D. Balkcom and M. Mason, "Time optimal trajectories for bounded velocity differential drive vehicles," *The International Journal of Robotics Research*, vol. 21, no. 3, pp. 199–217, 2002.
- [18] H. Chitsaz, S. LaValle, D. Balkcom, and M. Mason, "Minimum wheel-rotation paths for differential-drive mobile robots," *The International Journal of Robotics Research*, vol. 28, no. 1, pp. 66–80, 2009.
- [19] T. McGeer, "Passive dynamic walking," *The International Journal of Robotics Research*, vol. 9, no. 2, pp. 62–82, 1990.
- [20] M. J. Coleman, A. Chatterjee, and A. Ruina, "Motions of a rimless spoked wheel: a simple three-dimensional system with impacts," *Dynamics and Stability of Systems*, vol. 12, no. 3, pp. 139–159, 1997.
- [21] A. C. Smith and M. D. Berkemeier, "The motion of a finite-width rimless wheel in 3d," in *Robotics and Automation, 1998. Proceedings. 1998 IEEE International Conference on*, vol. 3. IEEE, 1998, pp. 2345–2350.
- [22] A. Bicchi, Y. Chitour, and A. Marigo, "Reachability and steering of rolling polyhedra: a case study in discrete nonholonomy," *Automatic Control, IEEE Transactions on*, vol. 49, no. 5, pp. 710–726, 2004.
- [23] L. Kronecker, *Näherungsweise ganzzahlige Auflösung linearer Gleichungen*, 1884.
- [24] J. Jahnel, "When is the (co) sine of a rational angle equal to a rational number?" *arXiv preprint arXiv:1006.2938*, 2010.
- [25] M. P. Do Carmo, *Differential geometry of curves and surfaces*. Prentice-Hall Englewood Cliffs, NJ, 1976, vol. 2.
- [26] A. V. Rao, D. A. Benson, C. Darby, M. A. Patterson, C. Franconin, I. Sanders, and G. T. Huntington, "Algorithm 902: Gpops, a matlab software for solving multiple-phase optimal control problems using the gauss pseudospectral method," *ACM Transactions on Mathematical Software*, vol. 37, no. 2, pp. 1–39, 2010.